Pluronic Triblock Copolymer Encapsulated Gold Nanorods as Biocompatible Localized Plasmon Resonance-Enhanced Scattering Probes for Dark-Field Imaging of Cancer Cells

ARTICLE *in* PLASMONICS · DECEMBER 2012

Impact Factor: 2.24 · DOI: 10.1007/s11468-012-9347-3

Plasmonics (2012) 7:595–601
DOI 10.1007/s11468-012-9347-3

Pluronic Triblock Copolymer Encapsulated Gold Nanorods as Biocompatible Localized Plasmon Resonance-Enhanced Scattering Probes for Dark-Field Imaging of Cancer Cells

Douglas Goh · Tianxun Gong · U. S. Dinish · Kaustabh Kumar Maiti · Chit Yaw Fu · Ken-Tye Yong · Malini Olivo

Received: 17 December 2011 / Accepted: 5 March 2012 / Published online: 18 March 2012

Abstract Gold nanorods (GNR) are synthesized using cetylmethylammonium bromide (CTAB) surfactants which function as structure-directing agents. However, CTAB forms a tightly bound cationic bilayer on GNR surface with the cationic trimethylammonium head group exposed to the aqueous media, which is known to be highly toxic in vitro and in vivo. Pluronic is a non-ionic triblock polymer, which can associate with CTAB and form stable CTAB–polymer complexes due to hydrophobic interactions. In this work, two types of Pluronic triblock copolymers were used to encapsulate GNR to reduce their cytotoxicity and improve colloidal and optical stability for biological applications. These formulations were characterized by UV–vis absorption spectra analysis, transmission electron microscopy, cell viability studies, differential interference contrast microscopy and dark-field imaging.

Keywords Gold nanorods · Plasmonic resonance · Pluronic encapsulation · CTAB–polymer complexes · Cytotoxicity · Colloidal and optical stability

Douglas Goh and Tianxun Gong contributed equally to this work.

Electronic supplementary material The online version of this article (doi:10.1007/s11468-012-9347-3) contains supplementary material, which is available to authorized users.

D. Goh · U. S. Dinish (✉) · K. K. Maiti · C. Y. Fu · M. Olivo (✉)
Bio-Optical Imaging Group, Singapore Bioimaging Consortium (SBIC), Agency for Science Technology and Research (A*STAR),
11 Biopolis Way,
Singapore 138667, Singapore
e-mail: Dinish@sbic.a-star.edu.sg
e-mail: Malini_olivo@sbic.a-star.edu.sg

T. Gong · K.-T. Yong (✉)
School of Electrical and Electronic Engineering,
Nanyang Technological University,
Singapore 639798, Singapore
e-mail: ktyong@ntu.edu.sg

M. Olivo
Bio-photonics group, School of Physics,
National University of Ireland,
Galway, Ireland

Introduction

Noble metal nanoparticles, especially gold nanoparticles, have received great interest in recent years as they possess many unique properties compared to those of bulk sizes. Fundamentally, they are capable of confining the resonant photons and induce coherent surface plasmon resonance (SPR) of their conduction band electrons, thus greatly enhancing their absorption and scattering properties [1]. Furthermore, the surfaces of these particles can be encapsulated with biomolecules for targeted delivery in vitro and in vivo. These unique electro-optical and chemical properties therefore allow the use of the nanoparticles in numerous applications such as photothermal therapy [2–4], photodynamic therapy [5], bio-imaging [6], biosensor [7], fluorescence enhancement [8], surface-enhanced Raman spectroscopy [9], drug delivery [10], etc. Over the past decade, various methods for the synthesis of gold nanoparticles of various shapes and sizes have been reported [11]. On one side, the SPR strongly depends on the shape and size of gold nanoparticles and can be easily tuned by changing those dimensions [12–14]. For isotropic nanoparticles such as nanospheres, SPR absorption peak is proportional to their diameter [14]. In the case of gold nanorods (GNR) with anisotropic shape, the SPR absorption peak splits into a transverse mode and a longitudinal mode corresponding to

the diameter and length of the rod, respectively [15, 16]. On the other side, for applications such as optical coherence tomography, photothermal therapy and photodynamic therapy, the SPR absorption peaks of nanoparticles can be tuned from 650 to 900 nm to optimize the light for tissue depth penetration [17]. Furthermore, cellular uptake of particulates can be up to 100 nm, and the optimum size is around 50 nm [18]. Considering all aforementioned facts, GNR are intriguing among all possible nanoparticle shapes as they have a high SPR tunability while maintaining a relatively small size compared to other nanoparticles.

GNR are synthesized with help of cetylmethylammonium bromide (CTAB) as a structure-inducing agent. However, it is suggested that CTAB forms a tightly bound cationic bilayer on GNR with the cationic trimethylammonium head group exposed to the aqueous media. CTAB exposure poses cytotoxicity to cells, thus limiting the use of GNR in biomedical applications [19, 20]. Reducing the cytotoxicity and enhancing the biocompatibility of GNR remain a great challenge for the last few years. Many methods were reported to reduce the cytotoxicity of the CTAB-coated GNR such as encapsulation of GNR with methoxy (polyethylene glycol)-thiol [21], bovine serum albumin and polyethylenimine [22] for biological applications.

In this work, we propose the encapsulation of GNR with Pluronic, a non-ionic triblock polymer that can associate with CTAB and form stable CTAB–polymer complexes due to hydrophobic interactions to reduce the cytotoxicity. These encapsulated GNR are characterized by UV–vis absorption spectra analysis and transmission electron microscopy (TEM). Subsequently, cell viability of oral squamous cell carcinoma (OSCC) cell line that is treated with these GNR is studied. We also report the use of Pluronic-encapsulated GNR as a biocompatible optical probe with capability for in vitro dark-field imaging.

Experimental

Materials

Hydrogen tetrachloroaurate(III) trihyrate ($HAuCl_4 \cdot 3H_2O$), CTAB, sodium borohydride (NH_4), silver nitrate ($AgNO_3$), L-ascorbic acid, Pluronic F108 and F127, trisodium citrate ($Na_3C_6H_5O_7$) and cell counting kit (CCK8) were purchased from Sigma-Aldrich. Dulbecco's modified Eagle medium (DMEM) and 1× phosphate buffer sulphate (PBS) were prepared in-house. Foetal bovine serum (FBS) and penicillin/streptomycin (Pen Strep) were purchased from Gibco®. Clean-mount solution to fix glass cover slip over eight-chamber slides was purchased from Electron Microscopy Sciences.

Gold Nanoparticle Seed Synthesis

Synthesis of gold seeds was adapted from Nikhoobakt et al. [23]. Briefly, 5 ml of 0.5 mM $HAuCl_4$ was added to 5 ml of 200 mM CTAB to obtain an amber-coloured solution. Six hundred microlitres of 10 mM $NaBH_4$ was then added to the solution and stirred vigorously for a minute. A light brown solution was obtained.

GNR Synthesis

Five millilitres of 1 mM $HAuCl_4$ was added to 5 ml of 200 mM CTAB and stirred. Three hundred fifty microlitres of 4 mM $AgNO_3$ was then added. Ninety microlitres of 80 mM of L-ascorbic acid was added, and a colourless solution was formed. Eighteen microlitres of the seed solution was injected into the growth solution and left to form GNR for an hour at room temperature. The GNR solution was centrifuged at 10,000 rpm for 10 min and suspended in water for a few times to remove excess unbounded CTAB.

Encapsulation of GNR with Pluronic

Pluronic solutions of corresponding types (F-108 and F-127) and concentrations (3, 5, 10, 20 and 30 mg/ml) were added to GNR solutions in one-to-one ratio and mixed. The resultant solutions were left to be incubated for 2 h and then centrifuged to remove excess Pluronic solutions. The encapsulated GNR were then resuspended in water. Concentrations of the solutions were fixed at optical density 1.5 with UV–vis spectrophotometer.

Gold Nanosphere Synthesis

Gold nanospheres are synthesized by the Turkevich method [24]. Nineteen millilitres of 0.526 mM $HAuCl_4$ was boiled while stirring. One millilitre of 30 mM $Na_3C_6H_5O_7$ was then added to the solution. Boiling was continued until 10 min after the solution turned wine red. The solution was cooled to room temperature and stored at 4 °C (Fig. S1, Electronic supplementary material).

TEM

TEM images to characterize the shapes and sizes of the GNR and gold nanospheres were taken with JEOL JEM-1010 operating at accelerating voltage of 80 kV. The specimens were prepared on 200-mesh nickel-coated TEM grids.

UV–Vis Absorption

UV–vis absorption spectra were obtained with Hitachi U-2900 with a double-beam optical system and spectral

bandpass of 1.5 nm over the spectrophotometric range of 400 to 1,100 nm. Specimen was placed in a quartz cuvette, and deionized water was used as a reference.

Cell Culture and Cell Viability

OSCC cell line was cultured in DMEM containing 10 % FBS with Pen Strep. All cultures were maintained at 37 °C with 5 % CO_2. Five thousand cells were seeded in a 96-well plate for 24 h before loading each well with 10 μl of corresponding synthesized GNR. After further incubating the cells for 24 h, 10 μl of CCK8 was added to each well and allowed to incubate for 4 h in dark at 37 °C with 5 % (*v*/*v*) CO_2. Cell population absorbance was performed with the SpectraMax 384 Plus spectral analyzer. The absorbance from the tetrazolium dye in CCK8 was measured at 450 nm excitation.

Sample Preparation for Dark-Field and Differential Interference Contrast Microscopy

Five thousand cells suspended in media were seeded in each well of the eight-well chamber glass slide and allowed to be confluent. Media were then removed, and the slide was rinsed with PBS. Media were replenished in the wells. The corresponding synthesized substances were loaded and allowed to incubate for 4 h at room temperature and pressure in dark. The media and synthesized substances were removed and rinsed with PBS again, and the cells were fixed with 4 % paraformaldehyde for 10 min. Thereafter, 4 % paraformaldehyde was removed and rinsed with PBS. The well was removed, and a cover slip was fastened with a layer of clean-mount on the slide.

Dark-Field Imaging

Dark-field imaging was performed with Nikon Eclipse 80i at 100× magnification, and local absorption spectra were analysed with the hyperspectral camera module.

Differential Interference Contrast Microscopy

Differential interference contrast microscopy was performed with Nikon A1 Confocal Microscope at 20× magnification powered with 405 nm laser to image DAPI-stained nuclei of cells.

Results and Discussion

GNR Synthesis and Encapsulation

We optimized the reported seed-mediated growth method [23] to synthesize GNR with TPR peak of 520 nm and LPR peak ranging from 750 to 800 nm with aspect ratio ~4 (Table S1, Electronic supplementary material). The GNR are grown from gold seeds and subsequent reduction of gold salt with a weak reducing agent (ascorbic acid) in a micellar medium [25]. For the formation of GNR, CTAB is an important ingredient and it was reported that CTAB head group can preferentially bind to the crystallographic faces of gold and acting as a structure-directing agent that "zips" up gold ions linearly to form the rod shape (Scheme 1a) [26]. Pluronic is a commercially synthesized non-ionic triblock polymer of a hydrophobic core chain of poly(propylene oxide) (PPO) sandwiched at its ends by two hydrophilic chains of poly(ethylene oxide). The hydrophobic PPO block of Pluronic can bind with the hydrophobic tail of CTAB and forming stable CTAB–polymer complexes (Scheme 1b) [27]. In comparison to CTAB, Pluronic presents higher biosafety since they have been approved by FDA for many years [28]. Two types of Pluronic, F-127 and F-108, were used to encapsulate GNR because they have longer PPO chains thus leading to better surface passivation and colloidal stability [29, 30].

As shown in Fig. 1a, Pluronic-encapsulated GNR exhibited no observable change in the UV–vis absorption spectra compared to the CTAB-coated GNR. Since the TPR and LPR peaks are determined by the diameter and length of the nanorods, the UV–vis absorption spectra suggest that the encapsulation of Pluronic on GNR did not alter the dimension. Furthermore, this was confirmed by the TEM images in Fig. 1b–d, where no change in dimension was observed for GNR before and after treatment with Pluronic. In addition, we also observed that passivation of Pluronic on the GNR surface can minimize blue shifting of LPR peak and suggests that they can stabilize GNR for long-term applications. CTAB-coated GNR exhibits ~20 nm blue shift, while Pluronic-encapsulated GNR shows only ~7 nm shift over 10 days, as shown in Fig. 2.

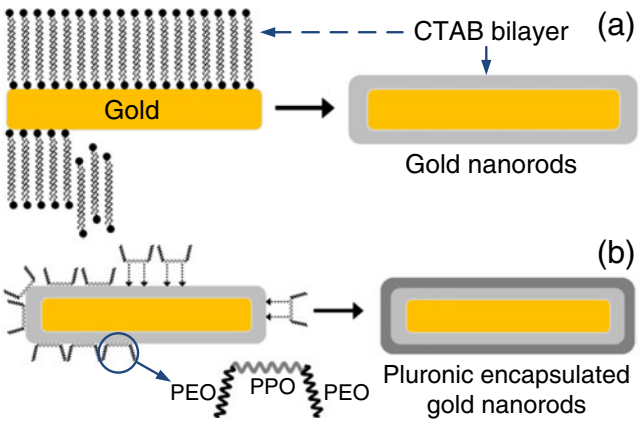

Scheme 1 **a** CTAB (*black squiggles*) as a structure-inducing agent during GNR formation as gold ions aggregate into an anisotropic rod (*yellow block*). **b** The PPO block of Pluronic binds with hydrophobic tail of CTAB by hydrophobic interactions and thus encapsulates GNR

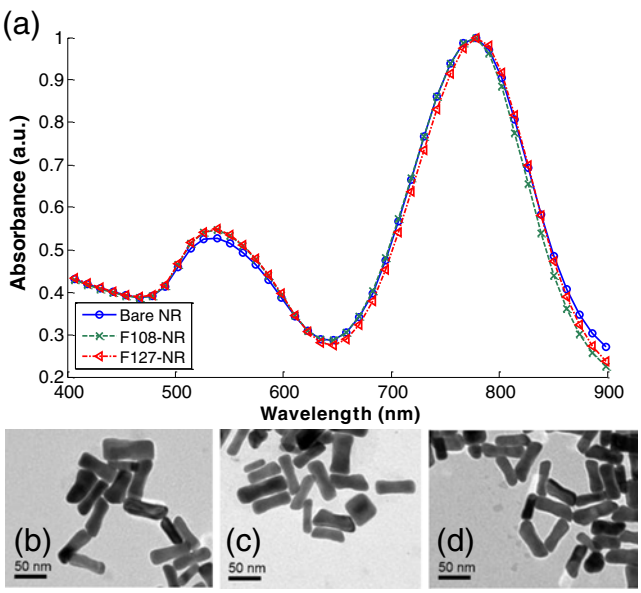

Fig. 1 **a** UV–vis spectra of CTAB-coated GNR (*Bare NR*), Pluronic F-108-encapsulated GNR (*F108-NR*) and Pluronic F-127-encapsulated GNR (*F127-NR*). The UV–vis spectra were taken from GNR suspended in HPLC water. TEM images of **b** Bare NR, **c** F108-NR and **d** F127-NR (concentration of Pluronic 20 mg/ml)

Cell Viability and DIC Microscopy

Cell viability tests were performed to evaluate the cytotoxicity of the Pluronic-encapsulated GNR using CCK assay with OSCC cell line. In this experiment, the CTAB-coated GNR were washed few times to remove excess unbounded CTAB before using them for the cell viability study. However, washing cannot remove the CTAB molecules bounded on the surface of GNR as indicated by relatively high cytotoxicity (70 % viability) as shown in Fig. 3a. On the contrary, gold nanospheres synthesized with trisodium citrate are non-toxic to the cells due to the citrate stabilization. In contrast, all the Pluronic-encapsulated GNR formulations maintained more than 80 % cell viability, even at

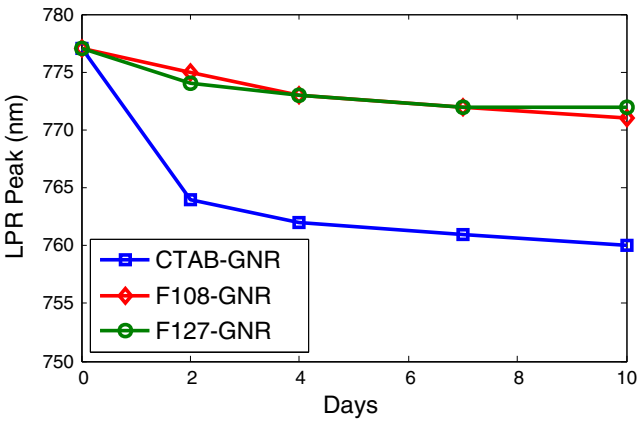

Fig. 2 Blue shifts trend with respect to the LPR peak of the absorption spectra of CTAB-coated GNR, F-108-coated GNR and F-127-coated GNR stored at room temperature over 10 days (concentration of Pluronic is 20 mg/ml)

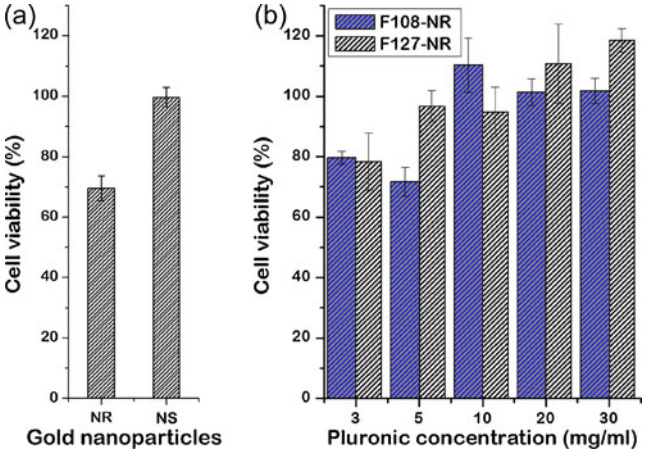

Fig. 3 **a** Cell viability of bare GNR (after centrifugation) and gold nanospheres (*NS*), **b** cell viability of Pluronic F-127 and F-108-encapsulated GNR with different Pluronic concentrations

Pluronic concentration as low as 3 mg/ml (Fig. 3b). This indicates that such Pluronic-encapsulated GNR can be used as efficient nanoprobes at non-cytotoxic dosages. The cells morphology images from the cell viability study are shown in Fig. 4 by using DIC microscopy. Figure 4a shows that the morphology of cells treated with CTAB-coated GNR and their flattened structure reveal that most cells are non-viable, while in Fig. 4b the rounded structure of cells shows that large amount of cells are viable. The cell viability study and DIC images not only confirm the cytotoxicity of the CTAB-coated GNR, thereby justifying our approach of the Pluronic triblock copolymer layering, but also demonstrate the biocompatibility of the Pluronic-encapsulated GNR formulations and highlighting their potential for in vitro imaging. It is worth noting that the viability of the cells treated with the F108 and F127 Pluronic-encapsulated GNR is more or less demonstrating the same biocompatibility.

Dark-Field Imaging

The Pluronic-encapsulated GNR formulation was then used as scattering probes [31] for cancer cells imaging. Previously, it was reported that nanoparticles encapsulated with Pluronic copolymers or PEG molecules were able to label the cells through non-specific uptake of the nanoparticles by the cells [32, 33]. In this study, the uptake of Pluronic-encapsulated GNR by OSCC cells was investigated using dark-field imaging. Figure 5a shows the control image of the OSCC cells without the addition of GNR.

In comparison, Fig. 5b, c with yellow/orange scattering colour dots within the cancer cells suggests that large quantity of Pluronic-functionalized GNR are internalized though non-specific uptake. In addition to dark-field imaging, the local absorption spectra analysis was performed on the cancer cells treated with Pluronic-encapsulated GNR. We have measured

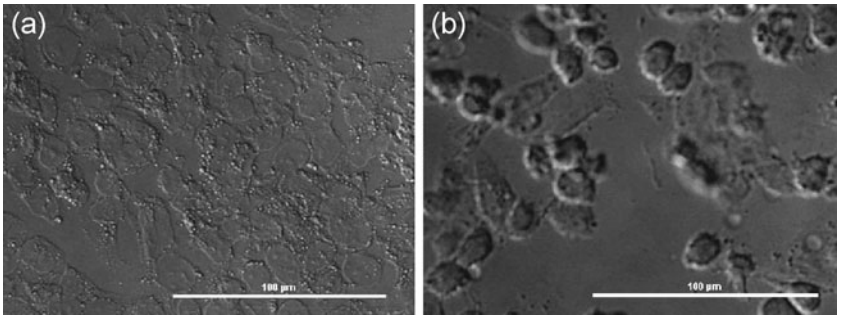

Fig. 4 DIC microscopy images depicting **a** OSCC cells treated with CTAB-coated GNR that are non-viable (flattened structure) and **b** OSCC cells treated with GNR encapsulated with F127 (30mg/ml) that are viable (rounded structure). This shows that CTAB-coated GNR are highly toxic to the cells while Pluronic-encapsulated GNR are highly biocompatible (*scale bar*=100 μm)

the yellow and orange scattering colour spots on the cancer cells using hyperspectra imaging analysis. TPR and LPR peaks observed from the measured hyperspectra in Fig. 5d, e confirm that the yellow/orange scattering colour spots originated from the Pluronic-encapsulated GNR. It is worth noting that a blue shift was observed for the SPR peaks from the hyperspectra as compared to the UV–vis spectra in Fig. 1a. This blue shift may be due to (1) different refractive index of the medium that causes the shift of SPR (UV–vis spectra were taken from GNR suspended in water while hyperspectra were taken from GNR on dry glass slide in air) [34] and (2) difference in the orientation of the GNR within the cells.

Conclusion

In summary, we have prepared GNR encapsulated with Pluronic F-108 and F-127 for in vitro dark-field imaging.

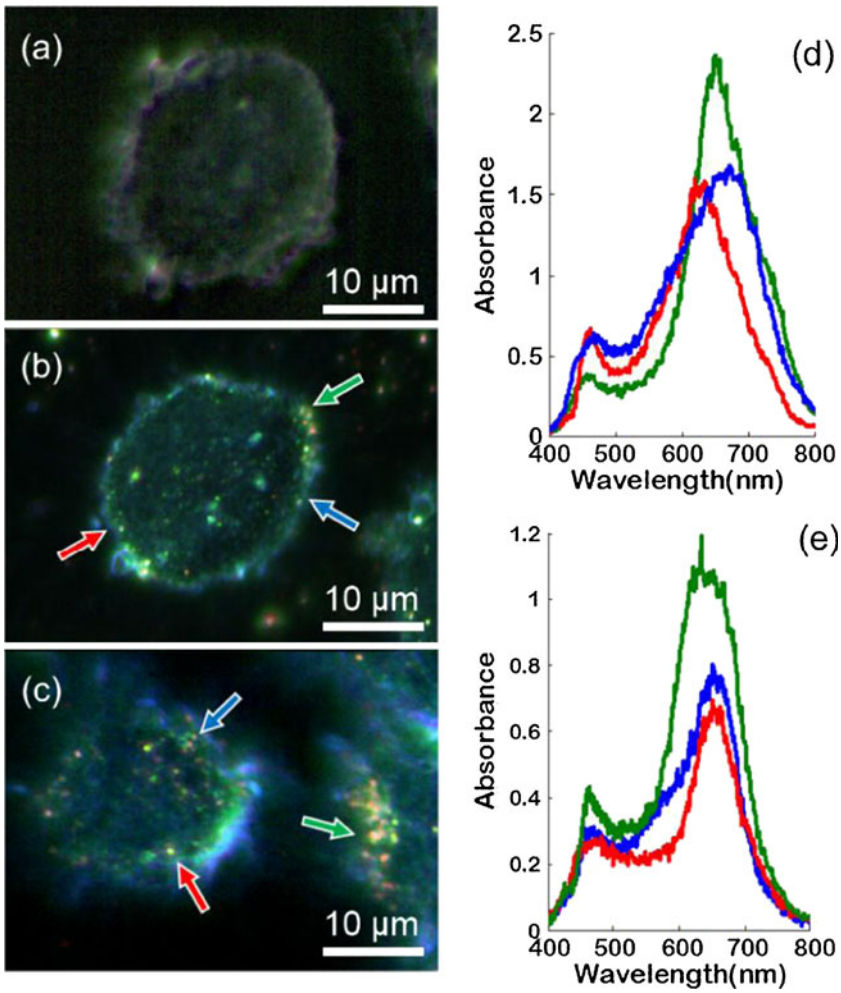

Fig. 5 Dark-field images of OSCC cells **a** without GNR, **b** uptaking of Pluronic F-108-encapsulated GNR and **c** uptaking of Pluronic F-127-encapsulated GNR. Hyperspectral absorption spectra of **d** F-127-encapsulated GNR (pointed out by arrows in Fig. 3b) and **e** F-108-encapsulated GNR (pointed out by arrows in Fig. 3c)

UV–vis spectra determine that the layering of Pluronic surfactants on the GNR surface did not change the dimension in comparison to the CTAB-coated GNR. In addition, the layering of Pluronic can significantly improve the colloidal and optical stability of GNR formulations. Pluronic-encapsulated GNR showed remarkably low cytotoxicity thus indicating their potential for in vitro imaging applications. Dark-field imaging and local hyperspectra analysis confirm the uptake of Pluronic-encapsulated GNR by the cancer cells. We believe that the prepared Pluronic-encapsulated GNR model herein can open many new opportunities towards the development of real-time in vivo GNR probes for photothermal imaging and photodynamic therapy.

Acknowledgments The authors would like to acknowledge Ms. Ching Tim Jang, attachment student from Nanyang Technological University, Singapore for her help in synthesis of gold nanorods, and SBIC Nikon Imaging Centre for their assistance in DIC imaging of the cells.

References

1. Eustis S, El-Sayed MA (2006) Why gold nanoparticles are more precious than pretty gold: noble metal surface plasmon resonance and its enhancement of the radiative and nonradiative properties of nanocrystals of different shapes. Chem Soc Rev 35(3):209–217
2. Jing-Liang L, Min G (2010) Gold-nanoparticle-enhanced cancer photothermal therapy. IEEE J Sel Top Quant Electron 16(4):989–996
3. Kim E, Yang J, Choi J, Suh JS, Huh YM, Haam S (2009) Synthesis of gold nanorod-embedded polymeric nanoparticles by a nano-precipitation method for use as photothermal agents. Nanotechnology 20(36). doi:10.1088/0957-4484/20/36/365602
4. Choi WI, Kim J-Y, Kang C, Byeon CC, Kim YH, Tae G (2011) Tumor regression in vivo by photothermal therapy based on gold-nanorod-loaded, functional nanocarriers. ACS Nano 5(3):1995–2003. doi:10.1021/nn103047r
5. Wieder ME, Hone DC, Cook MJ, Handsley MM, Gavrilovic J, Russell DA (2006) Intracellular photodynamic therapy with photosensitizer-nanoparticle conjugates: cancer therapy using a 'Trojan horse'. Photochem Photobiol Sci 5(8):727–734
6. Hsieh S, Meltzer S, Wang CRC, Requicha AAG, Thompson ME, Koel BE (2001) Imaging and manipulation of gold nanorods with an atomic force microscope. J Phys Chem B 106(2):231–234. doi:10.1021/jp012747x
7. David AS (2003) Plasmon resonant particles for biological detection. Curr Opin Biotechnol 14(1):13–22. doi:10.1016/s0958-1669(02)00015-0
8. Mohamed MB, Volkov V, Link S, El-Sayed MA (2000) The 'lightning' gold nanorods: fluorescence enhancement of over a million compared to the gold metal. Chem Phys Lett 317(6):517–523. doi:10.1016/s0009-2614(99)01414-1
9. Nikoobakht B, El-Sayed MA (2003) Surface-enhanced Raman scattering studies on aggregated gold nanorods†. J Phys Chem A 107(18):3372–3378. doi:10.1021/jp026770+
10. Paciotti GF, Myer L, Weinreich D, Goia D, Pavel N, McLaughlin RE, Tamarkin L (2004) Colloidal gold: a novel nanoparticle vector for tumor directed drug delivery. Drug Deliv 11(3):169–183. doi:10.1080/10717540490433895
11. Grzelczak M, Perez-Juste J, Mulvaney P, Liz-Marzan LM (2008) Shape control in gold nanoparticle synthesis. Chem Soc Rev 37(9):1783–1791
12. Gou L, Murphy CJ (2005) Fine-tuning the shape of gold nanorods. Chem Mater 17(14):3668–3672. doi:10.1021/cm050525w
13. Jana NR, Gearheart L, Murphy CJ (2001) Wet chemical synthesis of high aspect ratio cylindrical gold nanorods. J Phys Chem B 105(19):4065–4067. doi:10.1021/jp0107964
14. Hu M, Chen J, Li Z-Y, Au L, Hartland GV, Li X, Marquez M, Xia Y (2006) Gold nanostructures: engineering their plasmonic properties for biomedical applications. Chem Soc Rev 35(11):1084–1094
15. Prescott SW, Mulvaney P (2006) Gold nanorod extinction spectra. J Appl Phys 99(12):123504
16. Yong K-T, Sahoo Y, Swihart M, Schneeberger P, Prasad P (2008) Templated synthesis of gold nanorods (NRs): the effects of cosurfactants and electrolytes on the shape and optical properties. Top Catal 47(1):49–60. doi:10.1007/s11244-007-9030-7
17. Sharma P, Brown S, Walter G, Santra S, Moudgil B (2006) Nanoparticles for bioimaging. Adv Colloid Interface Sci 123–126:471–485. doi:10.1016/j.cis.2006.05.026
18. Chithrani BD, Ghazani AA, Chan WCW (2006) Determining the size and shape dependence of gold nanoparticle uptake into mammalian cells. Nano Lett 6(4):662–668. doi:10.1021/nl052396o
19. Murphy CJ, Gole AM, Stone JW, Sisco PN, Alkilany AM, Goldsmith EC, Baxter SC (2008) Gold nanoparticles in biology: beyond toxicity to cellular imaging. Acc Chem Res 41(12):1721–1730. doi:10.1021/ar800035u
20. Alkilany AM, Nagaria PK, Hexel CR, Shaw TJ, Murphy CJ, Wyatt MD (2009) Cellular uptake and cytotoxicity of gold nanorods: molecular origin of cytotoxicity and surface effects. Small 5(6):701–708. doi:10.1002/smll.200801546
21. Sanda CBS, Astilean (2010) Detoxification of gold nanorods by conjugation with thiolated poly(ethylene glycol) and their assessment as SERS-active carriers of Raman tags. Nanotechnology 21(235601):8. doi:10.1088/0957-4484/21/23/235601
22. Takahashi H, Niidome T, Kawano T, Yamada S, Niidome Y (2008) Surface modification of gold nanorods using layer-by-layer technique for cellular uptake. J Nanopart Res 10(1):221–228. doi:10.1007/s11051-007-9227-5
23. Nikoobakht B, El-Sayed MA (2003) Preparation and growth mechanism of gold nanorods (NRs) using seed-mediated growth method. Chem Mater 15(10):1957–1962. doi:10.1021/cm020732l
24. Turkevich J, Stevenson PC, Hillier J (1951) A study of the nucleation and growth processes in the synthesis of colloidal gold. Discuss Faraday Soc 11:55–75
25. Murphy CJ, Thompson LB, Chernak DJ, Yang JA, Sivapalan ST, Boulos SP, Huang J, Alkilany AM, Sisco PN (2011) Gold nanorod crystal growth: from seed-mediated synthesis to nanoscale sculpting. Curr Opin Colloid Interface Sci 16(2):128–134. doi:10.1016/j.cocis.2011.01.001
26. Pérez-Juste J, Pastoriza-Santos I, Liz-Marzán LM, Mulvaney P (2005) Gold nanorods: synthesis, characterization and applications. Coord Chem Rev 249(17–18):1870–1901. doi:10.1016/j.ccr.2005.01.030
27. Iqbal M, Chung Y-I, Tae G (2007) An enhanced synthesis of gold nanorods by the addition of Pluronic (F-127) via a seed mediated growth process. J Mater Chem 17(4):335–342
28. Sarwat FKS, Bhatia R, Susan CR (2005) Pluronic F127 as a cell encapsulation material: utilization of membrane-stabilizing agents. Tissue Eng 11(5–6):974–983. doi:10.1089/ten.2005.11.974
29. Sakai T, Alexandridis P (2006) Ag and Au monometallic and bimetallic colloids: morphogenesis in amphiphilic block copolymer solutions. Chem Mater 18(10):2577–2583. doi:10.1021/cm051757y
30. Sakai T, Alexandridis P (2004) Single-step synthesis and stabilization of metal nanoparticles in aqueous Pluronic block copolymer solutions at ambient temperature. Langmuir 20(20):8426–8430. doi:10.1021/la049514s

31. Wang SH, Lee CW, Chiou A, Wei PK (2010) Size-dependent endocytosis of gold nanoparticles studied by three-dimensional mapping of plasmonic scattering images. J Nanobiotechnology 8:33. doi:10.1186/1477-3155-8-33
32. Hawley AE, Illum L, Davis SS (1997) Lymph node localisation of biodegradable nanospheres surface modified with poloxamer and poloxamine block co-polymers. FEBS Lett 400(3):319–323. doi:10.1016/s0014-5793(96)01408-1
33. Reddy ST, Rehor A, Schmoekel HG, Hubbell JA, Swartz MA (2006) In vivo targeting of dendritic cells in lymph nodes with poly(propylene sulfide) nanoparticles. J Control Release 112(1):26–34. doi:10.1016/j.jconrel.2006.01.006
34. Mock JJ, Smith DR, Schultz S (2003) Local refractive index dependence of plasmon resonance spectra from individual nanoparticles. Nano Lett 3(4):485–491. doi:10.1021/nl0340475